Available online at www.sciencedirect.com
SCIENCE DIRECT®
Comput. Methods Appl. Mech. Engrg. 193 (2004) 4511–4539
Computer methods in applied mechanics and engineering
www.elsevier.com/locate/cma

The simple boundary element method for transient heat conduction in functionally graded materials

Alok Sutradhar, Glaucio H. Paulino *

Department of Civil and Environmental Engineering, University of Illinois at Urbana-Champaign, 2209 Newmark Laboratory, 205 North Mathews Avenue, Urbana, IL 61801-2352, USA

Received 31 July 2003; received in revised form 26 January 2004; accepted 9 February 2004

Abstract

This paper presents a "simple" boundary element method for transient heat conduction in functionally graded materials, which leads to a boundary-only formulation without any domain discretization. For a broad range of functional material variation (quadratic, exponential and trigonometric) of thermal conductivity and specific heat, the non-homogeneous problem can be transformed into the standard homogeneous diffusion problem. A three-dimensional boundary element implementation, using the Laplace transform approach and the Galerkin approximation, is presented. The time dependence is restored by numerically inverting the Laplace transform by means of the Stehfest algorithm. A number of numerical examples demonstrate the efficiency of the method. The results of the test examples are in excellent agreement with analytical solutions and finite element simulation results.

Keywords: Transient heat conduction; Boundary element method; Galerkin; Functionally graded materials; Non-homogeneous materials; Green's function; Three-dimensional analysis

1. Introduction

Recent advancements in material processing technology have enabled the design and manufacture of new material systems that can withstand very high temperatures and large temperature gradients. Functionally graded materials or FGMs are a new generation of composites where the volume fraction of the FGM constituents vary gradually, giving a non-uniform microstructure with continuously graded macroproperties such as heat conductivity, specific heat, density, etc. Typically, in an FGM, one face of a structural component is an engineering ceramic that can resist severe thermal loading and the other face is a metal which has excellent structural strength. FGMs consisting of heat-resisting ceramic and fracture-resisting metal can improve the properties of thermal barrier systems because cracking and delamination, which are often observed in conventional layered systems, are reduced by proper smooth transition of material properties. Ceramic based FGMs have also been used for thermal protection—see [1]. FGMs are

* Corresponding author. Tel.: +1-217-333-3817; fax: +1-217-265-8041.
E-mail address: paulino@uiuc.edu (G.H. Paulino).

0045-7825/$ - see front matter © 2004 Elsevier B.V. All rights reserved.
doi:10.1016/j.cma.2004.02.018

being developed as thermal barrier materials for combustion chambers, gas vanes, air vanes, nose cones, fuel valve sheets and piston crowns which undergo high-temperature gradient and high-thermal cycles in addition to wear. A comprehensive treatment of the science and technology of FGMs can be found, for example, in the books by Miyamoto et al. [2], Suresh and Mortensen [3], and the review article by Paulino et al. [4].

Among the numerical techniques for solution of engineering problems, the boundary element method (BEM) is a well-established and powerful method with good efficiency and accuracy. The efficiency arises because only the boundary is discretized and the accuracy comes from the fact that the Green's function is used as the weighting function in the formulation.

Steady state heat conduction in non-homogeneous media has been addressed by a few BEM researchers. Bialecki and Kuhn [7] presented a multi-zone approach where the material property was modeled as constant in certain zones in the layered media. Divo and Kassab [8] introduced a technique for heat conduction problems in heterogeneous media based on a fundamental solution that is a locally radially symmetric response to non-symmetric forcing functions. Shaw and Manolis [9] employed a conformal mapping technique to solve heat conduction problems in graded materials. Tanaka et al. [10] derived a dual reciprocity BEM formulation for FGMs. Gray et al. [11] developed a Galerkin BEM formulation by deriving the Green's function for steady state heat conduction problem in exponentially graded materials.

Transient heat conduction problems are usually solved using either the time domain approach or the Laplace transform domain approach. In the *time domain approach*, a time marching scheme associated with the BEM solution at each time step is used, and solutions are found directly in the time domain. An alternative is to employ a *transform space approach* wherein the time dependent derivative is eliminated in favour of an algebraic transform variable. However, once the differential system is solved in transform space, inverse transform is required to reconstitute the solution in the time domain. A review of these techniques can be found in [5,6] and the references therein.

Sutradhar et al. [6] extended the work of Ref. [11] to transient heat conduction for exponentially graded materials in three dimensions using the Laplace transform (LT) BEM. The implementation in Ref. [6] is a pure boundary-only formulation without any domain integral, however it relies on the actual Green's function (GF) associated with the function describing the material gradation. Recently, Sladek et al. [12–14] presented a meshless local boundary integral equation (LBIE) formulation for transient heat conduction considering exponential material variation. In the LBIE approach, the domain is divided into small circular sub-domains and on the surface of the sub-domains the LBIEs are written, resulting in a boundary-domain integral formulation. In each domain, the fundamental solution is related to the corresponding material constants. A different approach to treat transient heat conduction in non-homogeneous materials can be found in the book by Divo and Kassab [8].

Recently, Sutradhar and Paulino [15] proposed a simple three-dimensional (3D) BEM where non-homogeneous problems can be transformed to known homogeneous problems for a class of variations (quadratic, exponential and trigonometric) of thermal conductivity. The material property can have a functional variation in one, two or three dimensions. The present work extends the simple BEM concept of Ref. [15] to transient problems. In the present work, the material density (ρ) is considered constant, and the thermal conductivity and the specific heat have been chosen to have the same functional variation so that the thermal diffusivity κ [1] is constant, i.e.,

$$\kappa = \frac{k(\mathbf{x})}{\rho c(\mathbf{x})} \equiv \text{constant}. \tag{1}$$

[1] The symbols k and κ should not be confused. Note that k denotes thermal conductivity and κ denotes thermal diffusivity.

This approach has been followed by Sladek et al. [12–14] in developing BEM formulation for transient thermal problems in FGMs. Carslaw and Jaeger [17] have also assumed the same material variation for both $k(\mathbf{x})$ and $c(\mathbf{x})$ by considering functions of the power law type

$$k = k_0 x^n, \quad c = c_0 x^n, \tag{2}$$

and linear type

$$k = k_0(1 + \alpha x), \quad c = c_0(1 + \alpha x), \tag{3}$$

in which k_0, c_0 and α are constants. An example of thermal properties for an actual FGM can be found in the experimental work by Khor and Gu [16], who investigated functionally graded yttria-stabilized ZrO_2/NiCoCrAlY coatings. For this specific material system, the thermal diffusivity is not a constant. However, the assumption of constant thermal diffusivity in FGMs leads to a class of solvable problems, which allow development of a boundary-only integral equation formulation without any domain discretization. Moreover, this method can provide benchmark solutions to other numerical methods (e.g. FEM, meshless, partition of unity) and can provide valuable insight into the thermal behavior of FGMs.

By using variable transformations, the transient heat equation for FGMs can be converted to the known standard diffusion equation for three different classes of material variations (quadratic, exponential and trigonometric). The variable transformation approach has been previously studied for potential problems by Cheng [18,19], Shaw [20], Shaw and Gipson [21], El Harrouni et al. [22,23], and Li and Evans [24]. Based on these references, an alternative approach for the BEM formulation is the Green's function approach [6], where each different material variation requires a different fundamental solution. Thus, the kernels necessary for the BEM implementation for each case are different. As a result, separate computer codes are required to deal with individual functional variations. Moreover, if the treatment of singularity involves analytical integration, then the solution becomes more involved [25]. By means of the variable transformation approach, which consists of simple changes in the boundary conditions of existing homogeneous transient heat conduction computer codes, the solutions for non-homogeneous media with quadratic, exponential and trigonometric material variations can be obtained.

Notice that our previous work [6] was based on the GF approach which could only handle exponentially graded materials with unidimensional material variation; while the present work is based on the variable transform approach, which can handle three classes of material gradation (quadratic, exponential and trigonometric) with multi-dimensional material variation. Moreover, since the diffusion equation for non-homogeneous materials can be transformed to the diffusion equation for homogeneous materials by means of the simple BEM concept, standard available BEM codes can be used with elementary modifications. This nice feature was not possible with the former approach of Ref. [6]. The present manuscript describes how to do the modifications, which lead to a straightforward numerical implementation.

The remainder of this paper is organized as follows. The basic equations of the diffusion problem are described in Section 2. The Green's function for the FGM diffusion equation is derived in Section 3. In Section 4, the Laplace transform BEM formulation is presented. Section 5 discusses several aspects of the numerical implementation of the boundary integral analysis including the numerical inversion of the Laplace transform. Afterwards, some numerical examples are presented and verified in Section 6. Finally concluding remarks are provided in Section 7.

2. Basic equations and the simple BEM concept

The governing differential equation for the transient heat conduction is given by

$$\nabla \cdot (k(x,y,z)\nabla\phi) = \rho c(x,y,z)\frac{\partial \phi}{\partial t}, \tag{4}$$

where $\phi = \phi(x, y, z; t)$ is the temperature function, k is the thermal conductivity, c is the specific heat, and ρ is the density which is assumed to be constant. Two types of boundary conditions are prescribed. The Dirichlet condition for the unknown temperature ϕ is

$$\phi(x, y, z; t) = \overline{\phi}(x, y, z; t), \tag{5}$$

on boundary Σ_1 and the Neumann condition for its flux is

$$q(x, y, z; t) = -k(x, y, z)\frac{\partial \phi(x, y, z; t)}{\partial n} = \overline{q}(x, y, z; t), \tag{6}$$

on boundary Σ_2, where $\mathbf{n}$ is the unit outward normal to Σ_2. Here a bar over the quantity of interest means that it assumes a prescribed value. For a well-posed problem $\Sigma_1 \cup \Sigma_2 = \Sigma$ with Σ being the entire boundary. As the problem is time dependent, in addition to these boundary conditions, an initial condition at a specific time t_0 must also be prescribed. For simplicity, a zero initial temperature distribution has been considered, i.e.

$$\phi(x, y, z; t_0) = \phi_0(x, y, z) = 0. \tag{7}$$

A non-zero initial condition will introduce a domain integral in the formulation, which can be handled by domain integral techniques such as dual reciprocity method [26] or particular solution method [27].

By defining a variable

$$v(x, y, z) = \sqrt{k(x, y, z)}\phi(x, y, z), \tag{8}$$

Eq. (4) can be rewritten as

$$\nabla^2 v + \left(\frac{\nabla k(x, y, z) \cdot \nabla k(x, y, z)}{4k^2(x, y, z)} - \frac{\nabla^2 k(x, y, z)}{2k(x, y, z)} \right) v = \frac{\rho c(x, y, z)}{k(x, y, z)} \frac{\partial v}{\partial t} \tag{9}$$

or

$$\nabla^2 v + k'(x, y, z)v = \frac{\rho c(x, y, z)}{k(x, y, z)} \frac{\partial v}{\partial t}, \tag{10}$$

where

$$k'(\cdot) = \frac{\nabla k(\cdot) \cdot \nabla k(\cdot)}{4k^2(\cdot)} - \frac{\nabla^2 k(\cdot)}{2k(\cdot)}. \tag{11}$$

If the heat conductivity and the specific heat have the same functional variation, say e.g.,

$$k(x, y, z) = k_0 f(x, y, z), \tag{12}$$

and

$$c(x, y, z) = c_0 f(x, y, z), \tag{13}$$

respectively then by substituting these material expressions into Eq. (10), one obtains

$$\nabla^2 v + k'(x, y, z)v = \frac{1}{\kappa} \frac{\partial v}{\partial t}, \tag{14}$$

where the constant thermal diffusivity is given by

$$\kappa = \frac{k_0}{c_0 \rho}. \tag{15}$$

If k' is either zero or a constant, then by introducing another variable substitution

$$v = \mathrm{e}^{k'\kappa t}u, \tag{16}$$

one gets from Eq. (14)

$$\nabla^2 u = \frac{1}{\kappa}\frac{\partial u}{\partial t}. \tag{17}$$

This is the standard diffusion equation for homogeneous materials. If a material variation makes $k'(x,y,z)$ in Eq. (10) zero or constant, then the FGM transient heat conduction, Eq. (4), can be transformed into the standard homogeneous case given by, Eq. (17).

2.1. Material variations

- If $k'(x,y,z) = 0$, then $k(x,y,z)$ can be determined according to Eq. (11), i.e.

$$\frac{\nabla k \cdot \nabla k}{4k^2} - \frac{\nabla^2 k}{2k} = 0. \tag{18}$$

  In this case, if $k(\cdot)$ varies along the z-direction only, then one gets

$$k(z) = k_0(c_1 + c_2 z)^2 \text{ (Quadratic)}, \tag{19}$$

  where c_1 and c_2 are arbitrary constants and k_0 is a reference value for the function k.
- If $k'(x,y,z) = -\beta^2$, then $k(x,y,z)$ can be determined according to Eq. (11), i.e.

$$\frac{\nabla k \cdot \nabla k}{4k^2} - \frac{\nabla^2 k}{2k} = -\beta^2. \tag{20}$$

  If $k(\cdot)$ varies only with z, then

$$k(z) = k_0(a_1\mathrm{e}^{\beta z} + a_2\mathrm{e}^{-\beta z})^2 \text{ (Exponential)}, \tag{21}$$

  where a_1 and a_2 are arbitrary constants.
- If $k'(x,y,z) = \beta^2$, then $k(x,y,z)$ can be determined from Eq. (11), i.e.

$$\frac{\nabla k \cdot \nabla k}{4k^2} - \frac{\nabla^2 k}{2k} = \beta^2. \tag{22}$$

  Again, for $k(\cdot)$ varying only with z,

$$k(z) = k_0(a_1 \cos\beta z + a_2 \sin\beta z)^2 \text{ (Trigonometric)}, \tag{23}$$

  where a_1 and a_2 are arbitrary constants.

Notice that for quadratic, exponential and trigonometric variations of both heat conductivity and specific heat, the FGM transient problem can be transformed into a standard diffusion equation.

2.2. Multi-dimensional material variation

Although in the above discussion, the material properties vary only in one coordinate, the technique can be applied to materials varying in two or three coordinates as well. For instance, the general expression for material property variation in three dimensions are given below.

- Quadratic

$$k(x,y,z) = k_0(a_1 + a_2x)^2(b_1 + b_2y)^2(c_1 + c_2z)^2 \text{ and} \tag{24}$$

$$k_0(d_1 + d_2x + d_3y + d_4z + d_5xy + d_6yz + d_7zx + d_8xyz)^2. \tag{25}$$

Here a_1, a_2, b_1, b_2, c_1, c_2, and d_i $(i = 1, \ldots, 8)$ are arbitrary constants.

- Exponential

$$k(x,y,z) = k_0(a_1e^{\alpha x})^2(b_1e^{\beta y})^2(c_1e^{\gamma z})^2. \tag{26}$$

Here a_1, b_1, c_1, α, β and γ are arbitrary constants.

- Trigonometric

$$k(x,y,z) = k_0(a_1\cos\alpha x + a_2\sin\alpha x)^2(b_1\cos\beta y + b_2\sin\beta y)^2(c_1\cos\gamma z + c_2\sin\gamma z)^2. \tag{27}$$

Here a_1, a_2, b_1, b_2, c_1, c_2, α, β and γ are arbitrary constants. A numerical example with a 3D quadratic material variation is included in Section 6.

3. Green's function (GF)

The GF can be derived in closed form directly for the material property variations presented above because, by variable transformation the non-homogeneous problem can be transformed into a homogeneous problem for which the Green's function is known. The GF for the non-homogeneous problem is of great importance for a true boundary-only formulation.

The GF equation corresponding to Eq. (4) is

$$\nabla\cdot(k(x,y,z)\nabla G^*_{\mathrm{FGM}}) - \rho c(x,y,z)\frac{\partial G^*_{\mathrm{FGM}}}{\partial t} = -\delta(Q-P)\delta(t-t'), \tag{28}$$

where G^*_{FGM} is the GF, $\delta(Q-P)$ is the Dirac delta function located at the source point $P(x_P, y_P, z_P)$, and $Q(x,y,z)$ is the field point. By defining the variable $v = \sqrt{k(x,y,z)}G^*_{\mathrm{FGM}}$, and substituting in Eq. (28) one obtains

$$k^{1/2}(x,y,z)[\nabla^2 v + k'v] - \frac{\rho c(x,y,z)}{k^{1/2}(x,y,z)}\frac{\partial v}{\partial t} = -\delta(Q-P)\delta(t-t'). \tag{29}$$

After simplifying, one gets

$$\nabla^2 v + k'v - \frac{1}{\kappa}\frac{\partial v}{\partial t} = -\frac{\delta(Q-P)\delta(t-t')}{k^{1/2}(x_P,y_P,z_P)}, \tag{30}$$

where, due to the property of the Dirac delta function $\delta(Q-P)$, the independent variable of $k^{1/2}$ was changed from Q to P. If k' is either zero or a constant, then by defining another variable $u = e^{-k'\kappa t}v$ and using it in Eq. (30) we get

$$\nabla^2 u - \frac{1}{\kappa}\frac{\partial u}{\partial t} = -\frac{\delta(Q-P)\delta(t-t')}{k^{1/2}(x_P,y_P,z_P)e^{k'\kappa t}}. \tag{31}$$

Again, by the property of the Dirac delta function $\delta(t-t')$, a change in the independent variable t to t' is permissible, so that

$$\nabla^2 u - \frac{1}{\kappa}\frac{\partial u}{\partial t} = -\frac{\delta(Q-P)\delta(t-t')}{k^{1/2}(x_P,y_P,z_P)e^{k'\kappa t'}}. \tag{32}$$

The solution of the GF of Eq. (32) can be readily obtained as

$$u(P,Q) = G^*_{\text{hom}}(P,Q)k^{-1/2}(x_P,y_P,z_P)\mathrm{e}^{-k'\kappa t'}, \tag{33}$$

where $G^*_{\text{hom}}(P,Q)$ is the GF of the standard diffusion equation for the homogeneous problem. The GF corresponding to Eq. (30) is therefore,

$$v(P,Q) = \mathrm{e}^{k'\kappa t}u(P,Q) = G^*_{\text{hom}}(P,Q)k^{-1/2}(x_P,y_P,z_P)\mathrm{e}^{k'\kappa(t-t')}. \tag{34}$$

Similarly, the GF corresponding to Eq. (28) is

$$G^*_{\text{FGM}} = k^{-1/2}(x,y,z)v(P,Q) = G^*_{\text{hom}}(P,Q)k^{-1/2}(x,y,z)k^{-1/2}(x_P,y_P,z_P)\mathrm{e}^{k'\kappa(t-t')}. \tag{35}$$

The time dependent fundamental solution or the GF for the homogeneous problem is [17]

$$G^*_{\text{hom}}(P,Q) = \frac{1}{\left[4\pi\kappa(t-t')\right]^{3/2}}\mathrm{e}^{-\frac{r^2}{4\kappa(t-t')}}. \tag{36}$$

The GF represents the temperature field at time t produced by an instantaneous source of heat at point $P(x_P,y_P,z_P)$ at the time t', r is the distance between the source point P and the field point Q. The GF for the non-homogeneous material problem from Eq. (35) is therefore

$$G^*_{\text{FGM}}(P,Q) = \frac{\mathrm{e}^{-\frac{r^2}{4\kappa(t-t')}}}{\left[4\pi\kappa(t-t')\right]^{3/2}}\frac{\mathrm{e}^{k'\kappa(t-t')}}{k^{1/2}(x,y,z)k^{1/2}(x_P,y_P,z_P)}. \tag{37}$$

For the Laplace transform (LT) approach, the GF for the homogenous problem in the Laplace space is

$$G^*_{\text{hom}}(P,Q,s) = \frac{1}{4\pi r}\mathrm{e}^{-\sqrt{s/\kappa}r}. \tag{38}$$

Following the above procedure by incorporating the variable transformations, the GF for the non-homogeneous material problem in the LT space is derived as

$$G^*_{\text{FGM}}(P,Q,s) = \frac{1}{4\pi r}\frac{\mathrm{e}^{-\sqrt{-k'+\frac{s}{\kappa}}r}}{k(x,y,z)^{1/2}k(x_P,y_P,z_P)^{1/2}}. \tag{39}$$

Note that by setting $k'(x,y,z) = 0$, β^2 and $-\beta^2$, a quadratic, trigonometric and exponential material variation, respectively, can be obtained (See Table 1).

Although the GF for the FGM problem is given in this section, it is not used in the numerical implementation. Rather that using the GF for non-homogeneous materials, we employ the simple boundary element method concept of Ref. [15] and extend the concept to the transient case which allows us to use the standard GF, (Eqs. (36) and (38)), for homogeneous materials.

Table 1
Variable transformation approach

k'	Material variation	1D example
0	Quadratic	$k(z) = k_0(c_1 + c_2 z)^2$
β^2	Trigonometric	$k(z) = k_0(a_1\cos\beta z + a_2\sin\beta z)^2$
$-\beta^2$	Exponential	$k(z) = k_0(a_1\mathrm{e}^{\beta z} + a_2\mathrm{e}^{-\beta z})^2$

4. Laplace transform BEM (LTBEM) formulation

In the present work, the transformed approach is chosen. As explained in the previous sections, two variable transformations are used to reduce the non-homogeneous problem to the known standard diffusion problem. The first variable transformation involves only spatial variables (x, y, z) (from ϕ to v—see Eq. (8)) and the second variable transformation involves only the temporal variable t (from v to u—see Eq. (16)). Note that k' and κ are constants. The LTBEM formulation can be based on either variable u or variable v. In the following, the LTBEM formulations based on u and v are presented and their relative advantages and disadvantages are pointed out.

4.1. LTBEM formulation based on the variable u

Let the Laplace transform (LT) of u be denoted by

$$\tilde{u}(Q,s) = \int_{\mathscr{R}} u(Q,t)\mathrm{e}^{-st}\,\mathrm{d}t. \tag{40}$$

Here a tilde $\sim$ over a quantity of interest means LT of the quantity of interest. Thus, in LT space, the differential equation (17) becomes

$$\nabla^2\tilde{u} - \frac{s}{\kappa}\tilde{u} = 0, \tag{41}$$

where zero initial temperature ($u_0 = 0$ at $t = 0$) is considered for simplicity.

Following usual practice, the corresponding boundary integral statement can be obtained by 'orthogonalizing' this equation against an arbitrary (for now) function $f(x, y, z) = f(Q)$, and integrating over a bounded volume V

$$\int_V f(Q)\left(\nabla^2\tilde{u} - \frac{s}{\kappa}\tilde{u}\right)\mathrm{d}V_Q = 0. \tag{42}$$

According to Green's second identity, if the two functions ψ and λ have continuous first and second derivatives in V, then

$$\int_V (\psi\nabla^2\lambda - \lambda\nabla^2\psi)\mathrm{d}V = \int_\Sigma \left(\psi\frac{\partial\lambda}{\partial n} - \lambda\frac{\partial\psi}{\partial n}\right)\mathrm{d}S. \tag{43}$$

Using this relation and denoting the boundary of V by Σ, we obtain the first term of Eq. (42) as,

$$\int_V f(Q)\nabla^2\tilde{u}\mathrm{d}V_Q = \int_V \tilde{u}(Q)\nabla^2 f(Q)\mathrm{d}V_Q + \int_\Sigma \left(f(Q)\frac{\partial\tilde{u}(Q)}{\partial n} - \tilde{u}(Q)\frac{\partial f(Q)}{\partial n}\right)\mathrm{d}S_Q, \tag{44}$$

and using Eq. (43), we get,

$$0 = \int_\Sigma \left(f(Q)\frac{\partial\tilde{u}(Q)}{\partial n} - \tilde{u}(Q)\frac{\partial f(Q)}{\partial n}\right)\mathrm{d}S_Q + \int_V \tilde{u}(Q)\left(\nabla^2 f(Q) - \frac{s}{\kappa}f(Q)\right)\mathrm{d}V_Q, \tag{45}$$

where $n(Q) = (n_x, n_y, n_z)$ is the unit outward normal on Σ.

If we select $f(Q) = G(P, Q, s)$ as a GF, then the GF equation is

$$\nabla^2 G(P,Q,s) - \frac{s}{\kappa}G(P,Q,s) = -\delta(Q - P), \tag{46}$$

where δ is the Dirac delta function. Thus the source point volume integral in Eq. (45) becomes $-\tilde{u}(P)$. By means of Eq. (46), Eq. (45) can be rewritten as

$$\tilde{u}(P) + \int_{\Sigma} \left(\frac{\partial G(P,Q)}{\partial n} \right) \tilde{u}(Q) \mathrm{d}S_Q = \int_{\Sigma} G(P,Q) \frac{\partial \tilde{u}(Q)}{\partial n} \mathrm{d}S_Q. \tag{47}$$

Accordingly, the GF for the homogenous diffusion equation is given by Eq. (38) as

$$G(P,Q,s) = \frac{1}{4\pi r} \mathrm{e}^{-\sqrt{(s/\kappa)}r}. \tag{48}$$

4.2. Boundary conditions for formulation based on the variable u

In order to solve the boundary value problem based on the modified variable u, the boundary conditions of the original problem should be incorporated in the modified boundary value problem. Thus, for the modified problem, the Dirichlet and the Neumann boundary conditions change to the following form, respectively:

$$\overline{u} = \mathrm{e}^{-k'\kappa t}\overline{v} = \mathrm{e}^{-k'\kappa t}\sqrt{k}\,\overline{\phi}(Q,t) \quad \text{on } \Sigma_1, \tag{49}$$

$$\frac{\partial \overline{u}}{\partial n} = \frac{1}{2k}\frac{\partial k}{\partial n} u - \frac{\overline{q}(Q,t)}{\sqrt{k}} \mathrm{e}^{-k'\kappa t} \quad \text{on } \Sigma_2. \tag{50}$$

The boundary conditions must also be transformed into the Laplace space, i.e.

$$\tilde{\overline{u}} = \sqrt{k} \int_{\mathscr{R}} \overline{\phi}(Q,t) \mathrm{e}^{-k'\kappa t} \mathrm{e}^{-st} \mathrm{d}t, \tag{51}$$

$$\frac{\partial \tilde{\overline{u}}}{\partial n} = \frac{1}{2k}\frac{\partial k}{\partial n}\tilde{u} - \frac{1}{\sqrt{k}} \int_{\mathscr{R}} \overline{q}(Q,t) \mathrm{e}^{-k'\kappa t} \mathrm{e}^{-st} \mathrm{d}t. \tag{52}$$

4.3. LTBEM formulation based on the variable v

Let the Laplace transform (LT) of v be denoted by

$$\tilde{v}(Q,s) = \int_{\mathscr{R}} v(Q,t) \mathrm{e}^{-st} \mathrm{d}t. \tag{53}$$

If the formulation is based on the modified variable v instead of u, then the differential equation for the formulation instead of (41) becomes

$$\nabla^2 \tilde{v} + k'\tilde{v} - \frac{s}{\kappa}\tilde{v} = 0. \tag{54}$$

Following the same steps as before, the final form of the boundary integral formulation becomes

$$\tilde{v}(P) + \int_{\Sigma} \left(\frac{\partial G(P,Q)}{\partial n} \right) \tilde{v}(Q) \mathrm{d}S_Q = \int_{\Sigma} G(P,Q) \frac{\partial \tilde{v}(Q)}{\partial n} \mathrm{d}S_Q. \tag{55}$$

Here, the GF in the 3D LT space is given by

$$G(P,Q,s) = \frac{1}{4\pi r} \mathrm{e}^{-\sqrt{-k'+(s/\kappa)}r}. \tag{56}$$

Notice that the only difference between the formulations based on the variables u and v is in the Green's functions, Eq. (48) and Eq. (56), respectively. They differ in the exponential terms, i.e. $-\sqrt{-k'+s/\kappa}$ for the formulation based on v, and $-\sqrt{s/\kappa}$ for the formulation based on u. This change is very simple to

implement numerically in order to extend the homogeneous code for FGM problems. The change in the treatment of the boundary conditions for the formulation based on v is discussed below, and is employed in the present work.

4.4. Boundary conditions for formulation based on the variable v

The modified Dirichlet and Neumann boundary conditions for the modified variable v are

$$v = \sqrt{k}\,\overline{\phi}(Q,t) \quad \text{on } \Sigma_1, \tag{57}$$

and

$$\frac{\partial v}{\partial n} = \frac{1}{2k}\frac{\partial k}{\partial n}v - \frac{\overline{q}(Q,t)}{\sqrt{k}} \quad \text{on } \Sigma_2, \tag{58}$$

respectively. In the LT space they are transformed as

$$\tilde{v} = \sqrt{k}\,\tilde{\overline{\phi}}(Q,s) \quad \text{on } \Sigma_1, \tag{59}$$

and

$$\frac{\partial \tilde{v}}{\partial n} = \frac{1}{2k}\frac{\partial k}{\partial n}\tilde{v} - \frac{\tilde{\overline{q}}(Q,s)}{\sqrt{k}} \quad \text{on } \Sigma_2, \tag{60}$$

where

$$\tilde{\overline{\phi}}(Q,s) = \int_{\mathscr{R}} \overline{\phi}(Q,t)\mathrm{e}^{-st}\,\mathrm{d}t, \quad \tilde{\overline{q}}(Q,s) = \int_{\mathscr{R}} \overline{q}(Q,t)\mathrm{e}^{-st}\,\mathrm{d}t. \tag{61}$$

Compared to Eqs. (49)–(52), the changes herein do not involve an extra exponential function of t to deal with the Laplace transformation.

For constant values of $\overline{\phi}(Q,t)$ and $\overline{q}(Q,t)$, the expressions (59) and (60) becomes

$$\tilde{v} = \sqrt{k}\frac{\overline{\phi}(Q,t)}{s} \quad \text{on } \Sigma_1, \tag{62}$$

and

$$\frac{\partial \tilde{v}}{\partial n} = \frac{1}{2k}\frac{\partial k}{\partial n}\tilde{v} - \frac{\overline{q}(Q,s)}{s\sqrt{k}} \quad \text{on } \Sigma_2. \tag{63}$$

Notice that the Dirichlet boundary condition of the original problem is affected by the factor $\sqrt{k}$. Moreover, the Neumann boundary condition of the original problem changes to a mixed boundary condition or Robin boundary condition. This later modification is the only major change in the formulation.

Another common boundary condition of the original problem is a prescribed relationship between the potential and the flux (e.g. convective heat transfer problems). The boundary condition of this type is

$$q = \lambda_1\phi + \lambda_2 \text{ (Robin type)}. \tag{64}$$

The corresponding boundary condition for the modified problem is also a Robin boundary condition similar to Eq. (60), i.e.

$$\frac{\partial \tilde{v}}{\partial n} = \left(\frac{1}{2k}\frac{\partial k}{\partial n} - \lambda_1\right)\tilde{v} - \frac{\widetilde{\lambda_2}(Q,s)}{\sqrt{k}}. \tag{65}$$

4.5. Remarks

The formulation based on u uses the homogeneous GF, Eq. (48), but due to the exponential term $e^{-k'\kappa t}$, the modified boundary conditions in the LT space, Eqs. (51) and (52), include an exponential function of t in the Laplace transformation. On the other hand, the formulation based on v uses a slightly different Green's function (the exponential term changes from $-\sqrt{s/\kappa}$ to $-\sqrt{-k'+s/\kappa}$), but the treatment of the modified boundary condition does not involve the extra exponential term. For these reasons, we adopt the LTBEM formulation based on v for the numerical implementation. However, both formulations are equivalent.

5. Numerical implementation of the Galerkin LTBEM

The numerical methods employed in the current work use standard Galerkin techniques. A brief discussion of these techniques in the context of the BEM is presented below. It includes the development of the Galerkin boundary conditions (which is the main consideration in the simple BEM concept), selection of the boundary element type, treatment of singular integrals and corners, and numerical inversion of the Laplace transform in the LTBEM framework.

5.1. Galerkin boundary integral equation

Define the collocation BIE as

$$\mathscr{B}(P) \equiv \tilde{v}(P) + \int_{\Sigma} \left(\frac{\partial G(P,Q,s)}{\partial n} \right) \tilde{v}(Q) dQ - \int_{\Sigma} G(P,Q,s) \frac{\partial \tilde{v}(Q)}{\partial n} dQ \tag{66}$$

and thus for an exact solution $\mathscr{B}(P) \equiv 0$.

In a Galerkin approximation, the error in the approximate solution is orthogonalized against the shape functions, i.e. the shape functions are the weighting functions and the condition $\mathscr{B}(P) = 0$ is enforced in the 'weak sense', i.e.

$$\int_{\Sigma} N_k(P) \mathscr{B}(P) \mathrm{d}P = 0. \tag{67}$$

As a result the Galerkin technique possesses the important property of "local support" as illustrated by Fig. 1. The Galerkin technique is especially suitable to treat corners [28]. After replacing the boundary and the boundary functions by their interpolated approximations, a set of linear algebraic equations emerges,

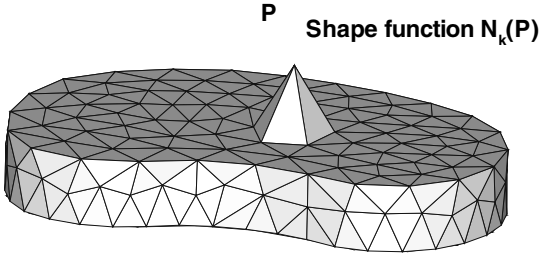

Fig. 1. The local support of the Galerkin formulation at the source point P.

$$[\mathbf{H}]\{\tilde{v}\} = [\mathbf{G}]\left\{\frac{\partial \tilde{v}}{\partial n}\right\}. \tag{68}$$

The matrix **G** is symmetric because its coefficients depend only on the distance (r) between the source point (P) and the field point (Q), but matrix **H** is not symmetric because it depends on the normal vector of the field point (Q). For Dirichlet problems, the Galerkin method gives rise to a symmetric system of equations.

After the boundary conditions of the problems are incorporated to the system, Eq. (68), the matrices can be reordered in the form

$$[\mathbf{A}]\{X\} = [\mathbf{B}], \tag{69}$$

where all the unknown quantities have been collected into the vector X. This system of equations can be solved by standard solution schemes for linear systems.

In the context of non-homogeneous media a symmetric Galerkin boundary element method (SGBEM) has been presented recently by Sutradhar et al. [25]. Details of the symmetry property and numerical implementation can be found in Refs. [29–31]. However, a non-symmetric Galerkin formulation, employing the singular Galerkin BIE, is adopted in the present work.

5.2. Treatment of boundary conditions

With respect to standard BEM codes the main modification in the implementation of the simple BEM is to incorporate the boundary conditions for the modified problem. In this section, the necessary modifications are described.

For the sake of illustration, let us assume three nodes, of which node 1 and node 3 have prescribed Neumann boundary condition, and node 2 has prescribed Dirichlet boundary condition, i.e.,

$\bar{q}_1, \quad \bar{\phi}_2, \quad \bar{q}_3$ known quantities,
$\phi_1, \quad q_2, \quad \phi_3$ unknown quantities.

These quantities are transformed into the Laplace space using Eq. (61). In the modified boundary value problem the variables are $\tilde{v}$ and $\partial\tilde{v}/\partial n$. The system of algebraic equations in the form of Eq. (68) emerges as,

$$\begin{bmatrix} H_{11} & H_{12} & H_{13} \\ H_{21} & H_{22} & H_{23} \\ H_{31} & H_{32} & H_{33} \end{bmatrix} \begin{Bmatrix} \tilde{v}_1 \\ \tilde{v}_2 \\ \tilde{v}_3 \end{Bmatrix} = \begin{bmatrix} G_{11} & G_{12} & G_{13} \\ G_{21} & G_{22} & G_{23} \\ G_{31} & G_{32} & G_{33} \end{bmatrix} \begin{Bmatrix} \partial\tilde{v}_1/\partial n \\ \partial\tilde{v}_2/\partial n \\ \partial\tilde{v}_3/\partial n \end{Bmatrix}. \tag{70}$$

By rearranging the equations so that the unknowns are passed to the left-hand side, we can rewrite the linear system as follows

$$\begin{bmatrix} H_{11} & -G_{12} & H_{13} \\ H_{21} & -G_{22} & H_{23} \\ H_{31} & -G_{32} & H_{33} \end{bmatrix} \begin{Bmatrix} \tilde{v}_1 \\ \partial\tilde{v}_2/\partial n \\ \tilde{v}_3 \end{Bmatrix} = \begin{bmatrix} G_{11} & -H_{12} & G_{13} \\ G_{21} & -H_{22} & G_{23} \\ G_{31} & -H_{32} & G_{33} \end{bmatrix} \begin{Bmatrix} \partial\tilde{v}_1/\partial n \\ \tilde{v}_2 \\ \partial\tilde{v}_3/\partial n \end{Bmatrix}. \tag{71}$$

Using Eqs. (59) and (60), we obtain the final form of the set of equations,

$$\begin{bmatrix} \left(H_{11} - \frac{G_{11}}{2k}\frac{\partial k}{\partial n}\right) & -G_{12} & \left(H_{13} - \frac{G_{13}}{2k}\frac{\partial k}{\partial n}\right) \\ \left(H_{21} - \frac{G_{21}}{2k}\frac{\partial k}{\partial n}\right) & -G_{22} & \left(H_{23} - \frac{G_{23}}{2k}\frac{\partial k}{\partial n}\right) \\ \left(H_{31} - \frac{G_{31}}{2k}\frac{\partial k}{\partial n}\right) & -G_{32} & \left(H_{33} - \frac{G_{33}}{2k}\frac{\partial k}{\partial n}\right) \end{bmatrix} \begin{Bmatrix} \tilde{v}_1 \\ \partial\tilde{v}_2/\partial n \\ \tilde{v}_3 \end{Bmatrix} = \begin{bmatrix} G_{11} & -H_{12} & G_{13} \\ G_{21} & -H_{22} & G_{23} \\ G_{31} & -H_{32} & G_{33} \end{bmatrix} \begin{Bmatrix} -\tilde{\bar{q}}_1(s)/\sqrt{k} \\ \tilde{\bar{\phi}}_2(s)\sqrt{k} \\ -\tilde{\bar{q}}_3(s)/\sqrt{k} \end{Bmatrix}, \tag{72}$$

which is in the form of Eq. (69). We solve these equations for $\tilde{v}_1$, $\partial\tilde{v}_2/\partial n$, and $\tilde{v}_3$; and finally, by using Eqs. (59) and (60), we obtain

$$\begin{aligned}
\tilde{\phi}_1(s) &= \tilde{v}_1/\sqrt{k},\\
\tilde{q}_2(s) &= -\sqrt{k}\left\{\frac{\partial\tilde{v}_2}{\partial n} - \frac{1}{2k}\frac{\partial k}{\partial n}\tilde{v}_2\right\},\\
\tilde{\phi}_3(s) &= \tilde{v}_3/\sqrt{k}.
\end{aligned} \tag{73}$$

These quantities are the solutions in the transform space. The final step is to invert this quantities back to the time domain by using numerical inverse Laplace transform technique.

5.3. Boundary elements

The surface of the solution domain is divided into a number of connected elements. Over each element, the variation of the geometry and the variables (potential and flux) is approximated by simple functions. Six-noded iso-parametric quadratic triangular elements are used (see Fig. 2).

The geometry of an element can be defined by the coordinates of its six nodes using appropriate quadratic shape functions as follows

$$x_i(\eta,\xi) = \sum_{j=1}^{6} N_j(\eta,\xi)(x_i)_j. \tag{74}$$

By means of an iso-parametric approximation, the same shape functions are used for the solution variables (both potential and flux), as follows

$$\begin{aligned}
\phi_i(\eta,\xi) &= \sum_{j=1}^{6} N_j(\eta,\xi)(\phi_i)_j,\\
q_i(\eta,\xi) &= \sum_{j=1}^{6} N_j(\eta,\xi)(q_i)_j.
\end{aligned} \tag{75}$$

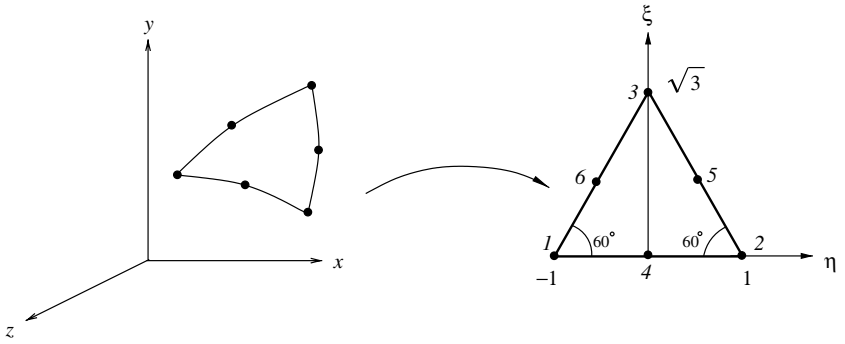

Fig. 2. A triangle in the 3D space is mapped to an equilateral triangular quadratic element in $\{\eta,\xi\}$ space, where $-1 \leqslant \eta \leqslant 1$, $0 \leqslant \xi \leqslant \sqrt{3}(1-|\eta|)$.

The shape functions can be explicitly written in terms of intrinsic coordinates ξ and η as (see Fig. 2):

$$\begin{aligned} N_1(\eta,\xi) &= (\xi+\sqrt{3}\eta-\sqrt{3})(\xi+\sqrt{3}\eta)/6, & N_4(\eta,\xi) &= (\xi+\sqrt{3}\eta-\sqrt{3})(\xi-\sqrt{3}\eta-\sqrt{3})/3, \\ N_2(\eta,\xi) &= (\xi-\sqrt{3}\eta-\sqrt{3})(\xi-\sqrt{3}\eta)/6, & N_5(\eta,\xi) &= -2\xi(\xi-\sqrt{3}\eta-\sqrt{3})/3, \\ N_3(\eta,\xi) &= \xi(2\xi-\sqrt{3})/3, & N_6(\eta,\xi) &= -2\xi(\xi+\sqrt{3}\eta-\sqrt{3})/3. \end{aligned} \tag{76}$$

The intrinsic coordinate space is the equilateral triangle with $-1 \leqslant \eta \leqslant 1$, $0 \leqslant \xi \leqslant \sqrt{3}(1-|\eta|)$.

5.4. Singular integrals

For three-dimensional problems, there are four typical configurations for the two elements containing the source point P and the field point Q (see Fig. 3), and thus four distinct situations regarding the singularity must be considered:

- *Non-singular case*, when the source point P and the field point Q lie on distinct elements, that do not share a common vertex or edge;
- *Coincident case*, when the source point P and the field point Q lie in the same element;
- *Edge adjacent case*, when two elements share a common edge; and
- *Vertex adjacent case*, when a vertex is the only common node between the two elements.

A hybrid analytical/numerical approach using the "limit to the boundary" approach has been adopted to treat the singular integrals. Details of this technique can be found in the papers by Gray et al. [32,33] and Sutradhar et al. [25].

5.5. Corners

The treatment of corners in the Galerkin BEM is simple and elegant due to the flexibility in choosing the weight function for the Galerkin approximation. Corners are represented by multiple nodes, and on each side different weight functions are used (see Fig. 4). For a mixed corner (flux is unknown in one side of the corner, potential is known), a non-zero weight function is assigned only on the side where flux is unknown.

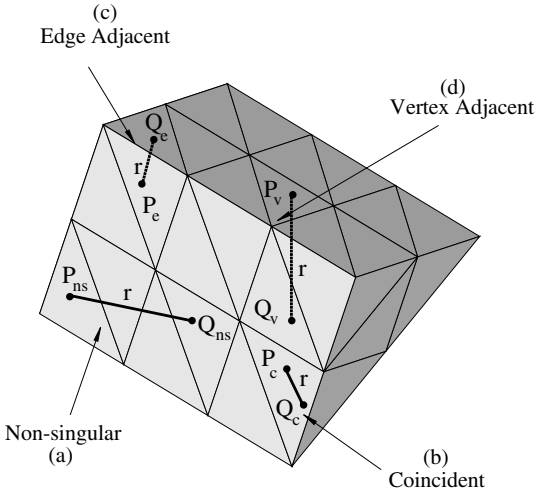

Fig. 3. Four different cases considered for integration: (a) non-singular; (b) coincident; (c) edge adjacent; and (d) vertex adjacent.

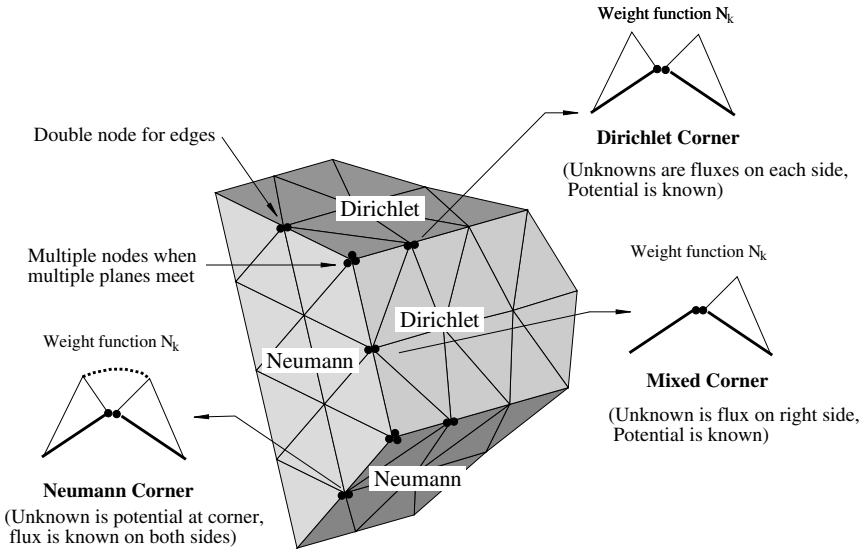

Fig. 4. Corner treatment in the Galerkin BEM.

For a Neumann corner (flux specified on both sides of the corner, potential is the unknown), the weight functions are combined together. On a Dirichlet corner (unknowns are flux on each sides, potential is known) the usual weight functions are assigned on both sides of the corners.

5.6. Numerical inversion of the Laplace transform

In the LTBEM approach, the numerical inversion of the LT is an important issue. For the present implementation the Stehfest's algorithm [34,35] has been employed for this purpose. Most of the methods for the numerical inversion of the LT require the use of complex values of the LT parameter, and as a result the use of complex arithmetic leads to additional storage and an increase in computation time. The disadvantage of using complex arithmetic has been overcome in Stehfest's method. It uses only real arithmetic and thus produces significant reduction in storage together with an increased efficiency in computation time. An useful discussion of the Stehfest's algorithm, in the BEM context, can be found in Sutradhar et al. [6] and Kassab and Divo [8].

If $\tilde{P}(s)$ is the Laplace transform of $F(t)$, then an approximate value F_a of the inverse $F(t)$ for a specific time $t = T$ is given by

$$F_a = \frac{\ln 2}{T} \sum_{i=1}^{N} V_i \tilde{P}\left(\frac{\ln 2}{T} i\right), \tag{77}$$

where

$$V_i = (-1)^{N/2+i} \sum_{k=\frac{i+1}{2}}^{\min(i,N/2)} \frac{k^{N/2}(2k)!}{(N/2-k)!k!(k-1)!(i-k)!(2k-i)!}. \tag{78}$$

Eqs. (77) and (78) correspond to the final form used in our numerical implementation.

When inverting a function from its Laplace transform, the results for different N should be compared to verify whether the function is smooth enough, to observe the accuracy, and to determine an optimum value

of N. Nordlund and Kassab [36] indicate that for sharp discontinuities in the temperature field the Stehfest's algorithm fails. In the present calculations, $N = 6$ was adopted after varying N from 6 to 10. Moridis and Reddell [37] and Zhu et al. [38] also found no significant change in their results for $6 \leqslant N \leqslant 10$.

During the inversion process, the sign of the expression under the square root in Eq. (56) i.e., $-\sqrt{-k' + s/\kappa}$ should not become negative. A few comments on this issue are in order. For the parabolic material variation $k' = 0$, and for the exponential material variation $k' = -\beta^2$. As a result for these two cases, the sign of the expression is always positive. However, for the trigonometric material variation, if $k' = \beta^2$ is greater than s/κ, then the sign can be negative, but it will depend on a few parameters. Since in the inversion process the Laplace parameter

$$s = \frac{\ln 2}{T} i, \tag{79}$$

where T is the specific time for which the solution is sought, there exists a criterion when the sign can be negative. The critical criterion can be written as

$$T > \frac{\ln 2}{\kappa \beta^2}, \tag{80}$$

which occurs for $i = 1$. The criterion depends on the relative magnitudes of the non-homogeneity parameter β, the specific time for solution T and the diffusivity κ.

6. Examples

In this section, a number of test examples are reported, demonstrating the implementation of the above techniques. To verify the numerical implementation, the following examples are presented:

(1) Cube problem
   - material gradation along the z-axis,
   - 3D material gradation.
(2) Rotor problem

The first example is a cube with constant temperatures in two sides and insulated in all the other sides. Two different cases are studied for this example by changing the material variation and changing the boundary conditions. For this problem, all the three kinds of material variation, i.e. quadratic, exponential and trigonometric, are prescribed. This is a verification problem, in which the numerical solutions are compared against analytical solutions. The other example is a rotor problem, which is of engineering significance in the field of functionally graded materials.

6.1. Cube problem

6.1.1. Material gradation along the z-axis

A unit cube ($L = 1$) with prescribed constant temperature on two sides is considered. The problem of interest and corresponding BEM mesh is shown in Fig. 5. The top surface of the cube at $[z = 1]$ is maintained at the temperature $T = 100$, while the bottom at $[z = 0]$ has $T = 0$. The remaining four faces are insulated (zero normal flux). The initial temperature is zero. Three different classes of variations are considered. Analytical solutions for the three cases are derived by using the method of separation of variables.

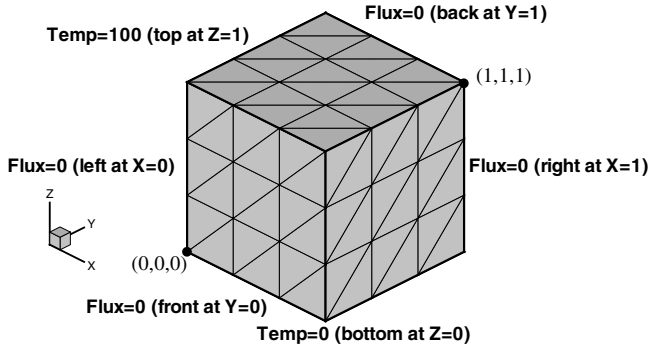

Fig. 5. Geometry and boundary conditions of the FGM unit cube problem with constant temperature on two planes. The BEM mesh consists of 294 nodes and 108 quadratic triangular elements.

Analytical solutions

- *Quadratic material gradation*

  Let the quadratic variation of thermal conductivity $k(x,y,z)$ and specific heat $c(x,y,z)$ be defined as

$$k(x,y,z) = k(z) = k_0(1+\beta z)^2 = 5(1+2z)^2, \tag{81}$$

  and

$$c(x,y,z) = c(z) = c_0(1+\beta z)^2 = 1(1+2z)^2, \tag{82}$$

  respectively, in which β is the non-homogeneity parameter. The analytical solution for temperature is

$$\phi(x,y,z;t) = \frac{T_1 z}{\sqrt{k}L} + \frac{2T_1}{\sqrt{k}}\sum_{n=1}^{\infty}\frac{\cos n\pi}{n\pi}\sin\frac{n\pi z}{L}\mathrm{e}^{-\left(\frac{n^2\pi^2}{L^2}\kappa t\right)}, \tag{83}$$

  where L is the dimension of the cube (in the z-direction) and

$$T_1 = \sqrt{k_0}(1+\beta L)T. \tag{84}$$

  The analytical solution for flux is

$$\begin{aligned} q(x,y,z;t) &= -k(x,y,z)\frac{\partial\phi}{\partial z} \\ &= -k(x,y,z)\left[\frac{(1+\beta L)T}{(1+\beta z)^2 L} + \frac{2T_1}{\sqrt{k}}\sum_{n=1}^{\infty}\frac{\cos n\pi}{n\pi}\sin\frac{n\pi z}{L}\mathrm{e}^{-\left(\frac{n^2\pi^2}{L^2}\kappa t\right)}\left(\cos\left(\frac{n\pi z}{L}\right)\frac{n\pi}{L}\right.\right. \\ &\quad \left.\left. - \sin\left(\frac{n\pi z}{L}\right)\frac{\beta}{(1+\beta z)}\right)\right]. \end{aligned} \tag{85}$$

- *Exponential material gradation*

  Let the exponential variation of thermal conductivity $k(x,y,z)$ and specific heat $c(x,y,z)$ be defined as

$$k(x,y,z) = k(z) = k_0\mathrm{e}^{2\beta z} = 5\mathrm{e}^{2z}, \tag{86}$$

  and

$$c(x,y,z) = c(z) = c_0\mathrm{e}^{2\beta z} = 1\mathrm{e}^{2z}, \tag{87}$$

respectively, where β is the non-homogeneity parameter. The analytical solution for temperature is

$$\phi(x,y,z;t) = T\frac{1-\mathrm{e}^{-2\beta z}}{1-\mathrm{e}^{-2\beta L}} + \sum_{n=1}^{\infty} \frac{2T\mathrm{e}^{\beta L} n\pi\cos n\pi}{\beta^2 L^2 + n^2\pi^2} \sin\frac{n\pi z}{L} \mathrm{e}^{-\beta z} \mathrm{e}^{-\left(\frac{n^2\pi^2}{L^2}+\beta^2\right)\kappa t}, \tag{88}$$

where L is the dimension of the cube (in the z-direction). The analytical solution for flux is

$$\begin{aligned} q(x,y,z;t) &= -k(x,y,z)\frac{\partial\phi}{\partial z} \\ &= -k(x,y,z)\left[\frac{2\beta T\mathrm{e}^{-2\beta z}}{1-\mathrm{e}^{-2\beta L}} + \sum_{n=1}^{\infty} \frac{2T\mathrm{e}^{\beta L} n\pi\cos n\pi}{\beta^2 L^2 + n^2\pi^2} \mathrm{e}^{-\beta z} \mathrm{e}^{-\left(\frac{n^2\pi^2}{L^2}+\beta^2\right)\kappa t} \left(\frac{n\pi}{L}\cos\frac{n\pi z}{L} - \beta\sin\frac{n\pi z}{L}\right)\right]. \end{aligned} \tag{89}$$

- *Trigonometric material gradation*
  Let the trigonometric variation of the thermal conductivity $k(x,y,z)$ and specific heat $c(x,y,z)$ be defined as

$$k(z) = k_0(a_1\cos\beta z + a_2\sin\beta z)^2 = 5(\cos(0.2z) + 2\sin(0.2z))^2, \tag{90}$$

  and

$$c(z) = c_0(a_1\cos\beta z + a_2\sin\beta z)^2 = 1(\cos(0.2z) + 2\sin(0.2z))^2, \tag{91}$$

  respectively, where β is the non-homogeneity parameter and a_1 and a_2 are constants. The analytical solution for temperature is

$$\phi(x,y,z;t) = \frac{T_1\sin\beta z}{\sqrt{k}\sin\beta L} + \frac{2T_1}{\sqrt{k}} \sum_{n=1}^{\infty} \frac{n\pi\cos n\pi}{n^2\pi^2 - \beta^2 L^2} \sin\frac{n\pi z}{L} \mathrm{e}^{-\left(\frac{n^2\pi^2}{L^2}-\beta^2\right)\kappa t}, \tag{92}$$

  where L is the dimension of the cube (in the z-direction) and

$$T_1 = \sqrt{k_0}(\cos\beta L + 2\sin\beta L)T. \tag{93}$$

  The analytical solution for flux is

$$\begin{aligned} q(x,y,z;t) &= -k(x,y,z)\frac{\partial\phi}{\partial z} \\ &= -k(x,y,z)\left[-\frac{(\cot\beta L + 2)T\beta}{3\cos^2\beta z - 4\cos\beta z\sin\beta z - 4} + \frac{2T_1}{\sqrt{k}} \sum_{n=1}^{\infty} \frac{n\pi\cos n\pi}{n^2\pi^2 - \beta^2 L^2} \right. \\ &\quad \left. \times \mathrm{e}^{-\left(\frac{n^2\pi^2}{L^2}-\beta^2\right)\kappa t} \left(\cos\left(\frac{n\pi z}{L}\right)\frac{n\pi}{L} - \sin\left(\frac{n\pi z}{L}\right)\frac{\beta(-\sin\beta z + 2\cos\beta z)}{(\cos\beta z + 2\sin\beta z)}\right)\right]. \end{aligned} \tag{94}$$

Results. The cube is discretized with 294 nodes and 108 quadratic triangular elements as illustrated by Fig. 5. The profiles of the thermal conductivity $k(z)$ of the three cases are illustrated in Fig. 6. The temperature profile along the z-axis is plotted at different times for the quadratic, exponential and trigonometric material variations, and compared with the analytical solutions in Figs. 7–9 respectively. The variation of flux at the $z = 0$ surface with respect to time is plotted in Fig. 10 for the three material variations. The variation of flux at the $z = 1$ surface is plotted in Fig. 11. The numerical and analytical results are in excellent agreement.

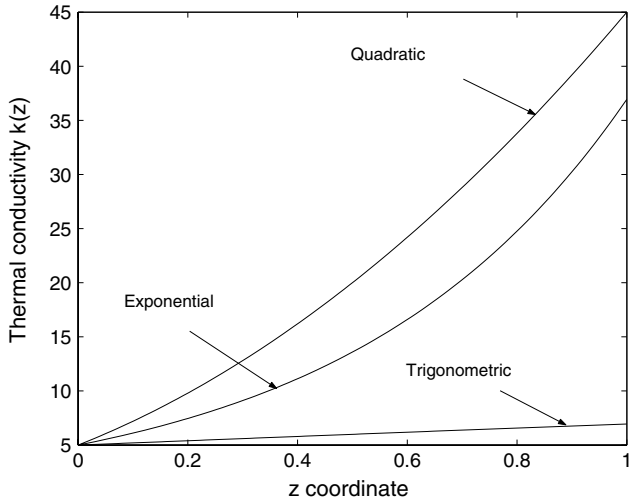

Fig. 6. Thermal conductivity variation along the z-direction. The quadratic variation is $k(z) = 5(1 + 2z)^2$, the exponential variation is $k(z) = 5e^{2z}$ and the trigonometric variation is $k(z) = 5[\cos(0.2z) + 2\sin(0.2z)]^2$.

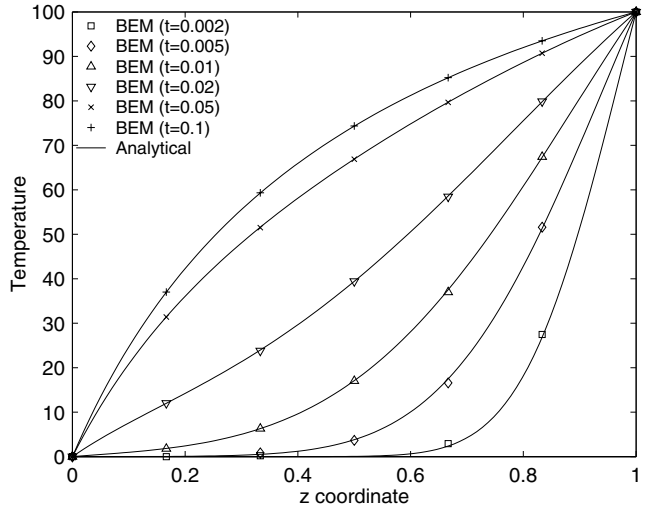

Fig. 7. Temperature profile in the z-direction for different time levels for the FGM cube problem with quadratic material variation.

6.1.2. Cube with three-dimensional material gradation

The three-dimensional variation of the thermal conductivity and the specific heat are

$$k(x, y, z) = (5 + 0.2x + 0.4y + 0.6z + 0.1xy + 0.2yz + 0.3zx + 0.7xyz)^2, \tag{95}$$

and

$$c(x, y, z) = 0.2(5 + 0.2x + 0.4y + 0.6z + 0.1xy + 0.2yz + 0.3zx + 0.7xyz)^2, \tag{96}$$

respectively. Fig. 12 illustrates the iso-surfaces of the three-dimensional variation of the thermal conductivity. The BEM mesh and the boundary conditions are shown in Fig. 13.

The initial temperature of the cube is kept as zero. The mixed boundary conditions at the six faces of the cube are prescribed as follows

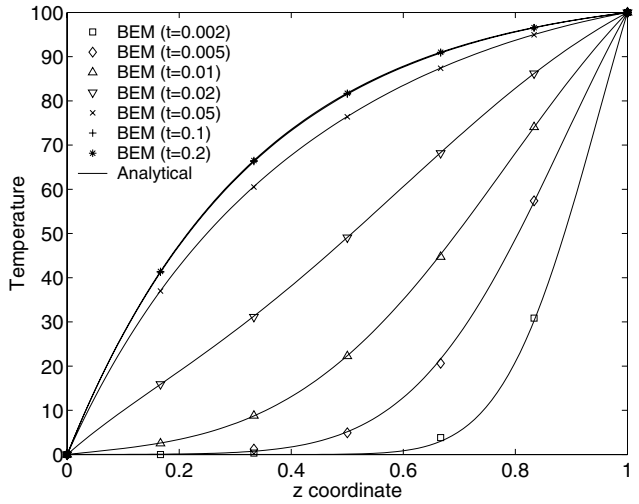

Fig. 8. Temperature profile in the z-direction for different time levels for the FGM cube problem with exponential material variation.

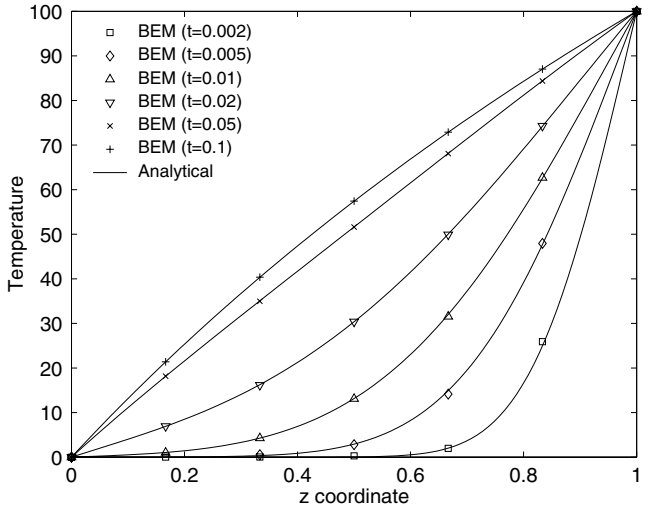

Fig. 9. Temperature profile in the z-direction for different time levels for the FGM cube problem with trigonometric material variation.

$$
\begin{aligned}
&\phi(0,y,z) = 0,\\
&\overline{q}(1,y,z) = -k(1,y,z)\frac{\partial\phi(x,y,z)}{\partial x} = -0.2zy(25+2y+3z+zy),\\
&\phi(x,0,z) = 0,\\
&\overline{q}(x,1,z) = -k(x,1,z)\frac{\partial\phi(x,y,z)}{\partial y} = -0.1xz(50+2x+6z+3xz),\\
&\phi(x,y,0) = 0,\\
&\overline{q}(x,y,1) = -k(x,y,1)\frac{\partial\phi(x,y,z)}{\partial z} = -0.1xy(50+2x+4y+xy).
\end{aligned}
\tag{97}
$$

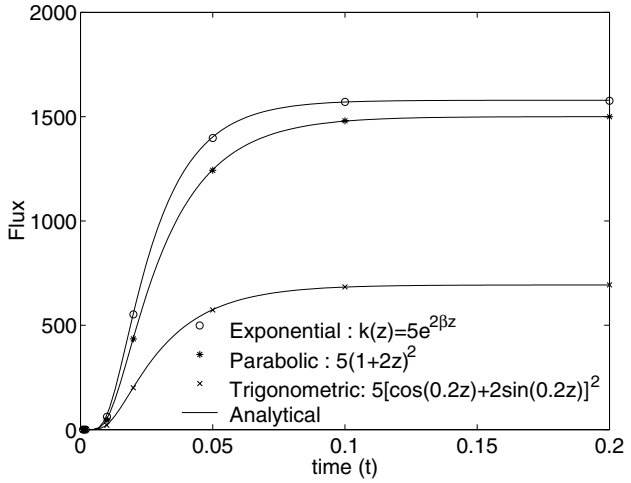

Fig. 10. Variation of flux at $z = 0$ surface with time for the three variations.

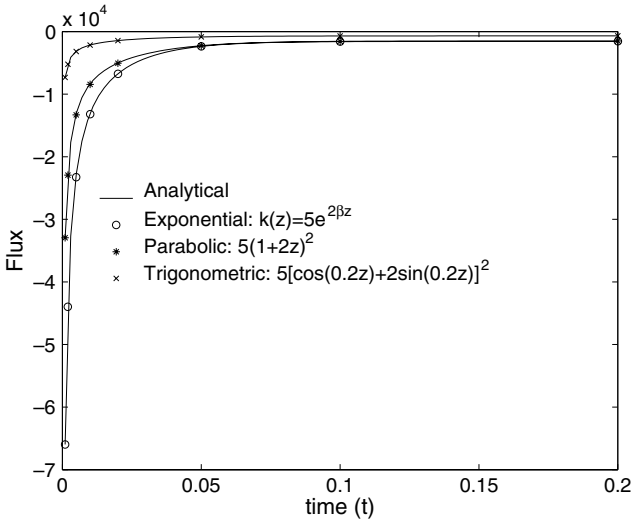

Fig. 11. Variation of flux at $z = 1$ surface with time for three types of material gradation.

The cube is discretized with 294 nodes and 108 quadratic triangular elements. For verification purposes, the BEM result is compared with the finite element simulation performed by the commercially available software ABAQUS. In the FEM simulation 4961 nodes and 1000 20-noded brick elements were used. The temperatures at $(1, 1, 1)$ and $(0.5, 1, 0.5)$ (center of the $Y = 1$ plane) are plotted against time and compared in Fig. 14. The results show good agreement. Note that the point of interest at $(1, 1, 1)$ is a corner node with Neumann boundary condition in all three associated planes and only three elements are used in each direction in the cube. Flux values at $(0.5, 0, 0.5)$ (center of the $Y = 0$ plane) are plotted against time and compared with the corresponding FEM solution in Fig. 15. These results are also in very good agreement. In general, conventional FEM software (including ABAQUS [39]) use homogeneous elements with

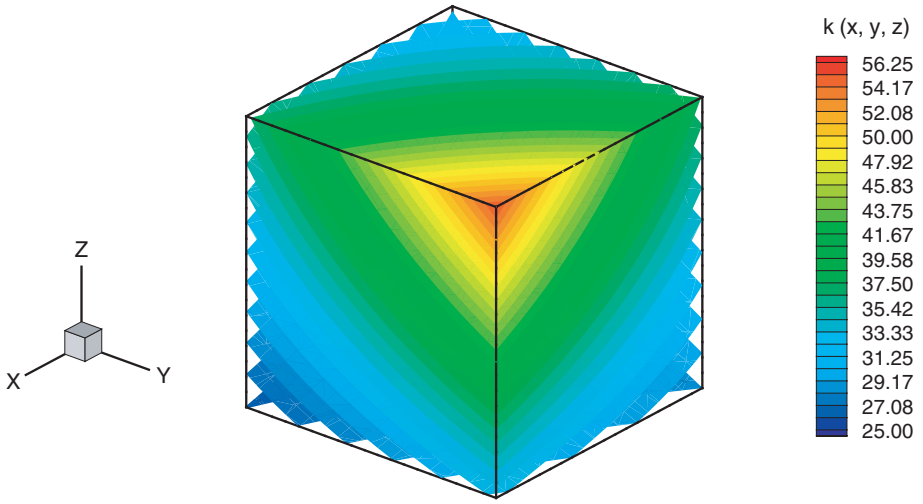

Fig. 12. Representation of iso-surfaces for the three-dimensional variation of thermal conductivity $k \equiv k(x, y, z)$.

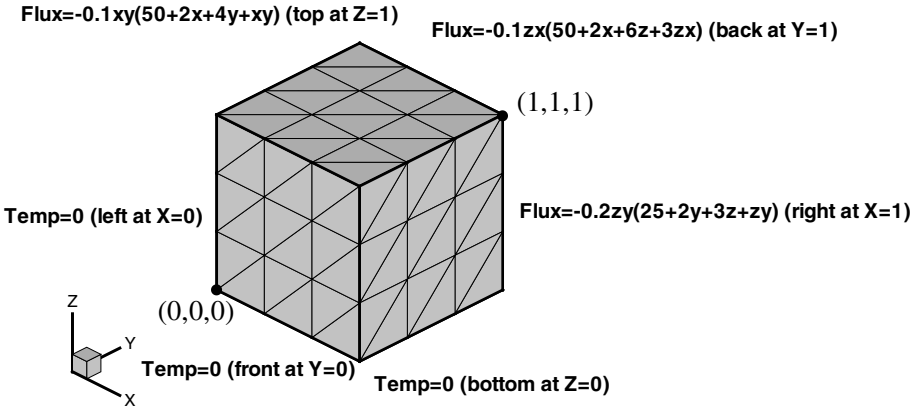

Fig. 13. The geometry, boundary conditions and the BEM mesh of the FGM unit cube problem with 3D material variation.

constant material properties at the element level. In order to incorporate the functional variation of the material at the finite element level, a user subroutine UMATHT [15] was developed for ABAQUS [39]. By means of this sub-routine, functional variations of thermal conductivity and specific heat can be included within an element by sampling the material property at each Gauss point. Graded elements approximate the material gradient better than conventional homogeneous elements and provide a smoother transition at element boundaries. Further investigations on graded elements can be found in the papers by Santare and Lambros [40] and Kim and Paulino [41] for 2D problems, and in the paper by Walters et al. [42] for 3D problems.

6.2. Rotor problem

The last numerical example is an FGM rotor with eight mounting holes having an eightfold symmetry. Due to the symmetry, only one-eighth of the rotor is analysed. The top view of the rotor, the analysis

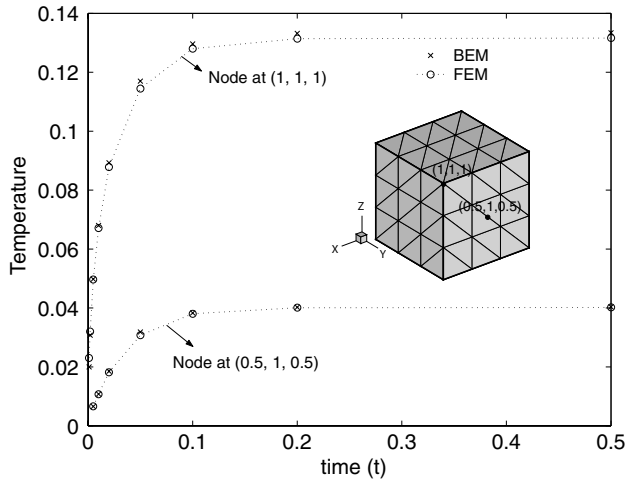

Fig. 14. Variation of temperature with time at $(1, 1, 1)$ and $(0.5, 1, 0.5)$.

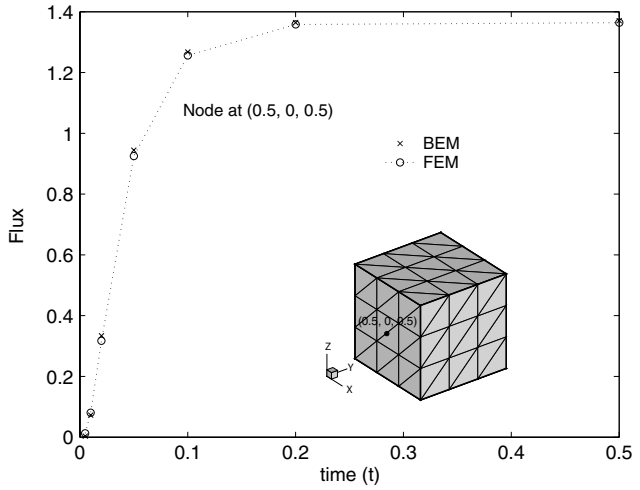

Fig. 15. Variation of flux with time at $(0.5, 0, 0.5)$.

region, and the geometry of the region are illustrated in Fig. 16. The grading direction for the rotor is parallel to its line of symmetry, which is taken as the z-axis.

The thermal conductivity and the specific heat for the rotor vary quadratically according to,

$$k(z) = 20(1 + 420.7z)^2, \tag{98}$$

and

$$c(z) = 5(1 + 420.7z)^2, \tag{99}$$

respectively.

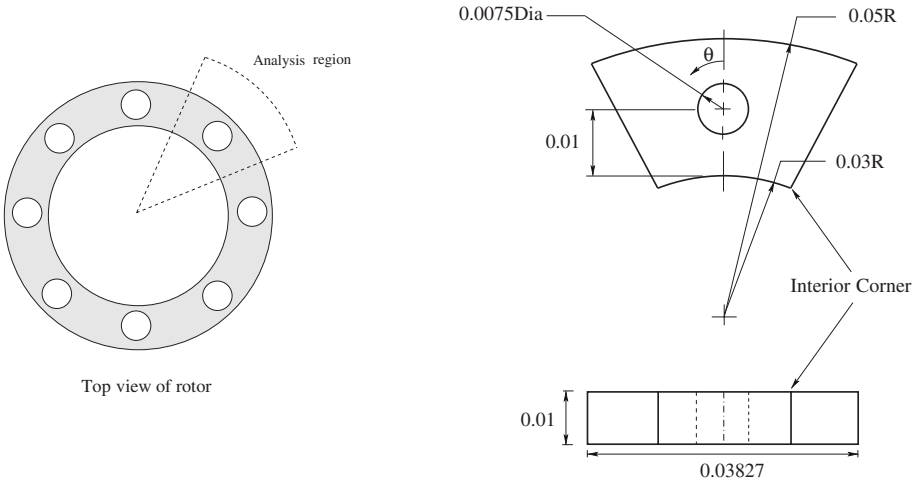

Fig. 16. Geometry of the functionally graded rotor with eightfold symmetry.

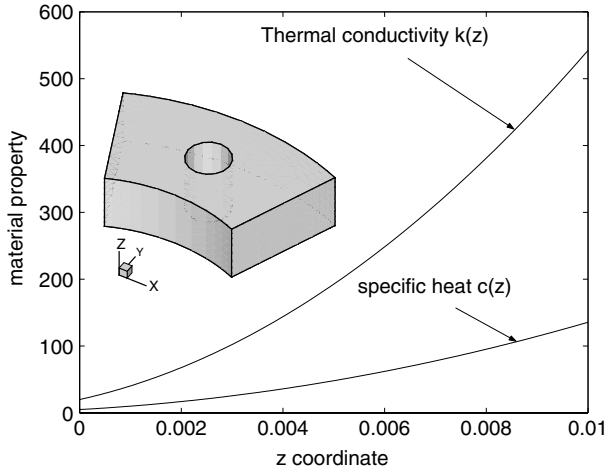

Fig. 17. Profile of thermal conductivity and specific heat along z-direction. The quadratic variation of the thermal conductivity and specific heat are $k(z) = 20(1 + 420.7z)^2$ and $c(z) = 5(1 + 420.7z)^2$, respectively.

The profile of the thermal conductivity $k(z)$ and the specific heat $c(z)$ of the variations are illustrated in Fig. 17. The temperature is specified along the inner radius as $T_{\text{inner}} = 20 + 1.25 \times 10^6(z - 0.01)^2$ and outer radius as $T_{\text{outer}} = 150 + 1.25 \times 10^6(z - 0.01)^2$. A uniform heat flux of 5×10^5 is added on the bottom surface where $z = 0$, and all the other surfaces are insulated. The BEM mesh employs 1584 elements and 3492 nodes. A schematic for the thermal boundary conditions and the BEM mesh employed is shown in Fig. 18. Here the solution of the problem is verified with the commercially available software ABAQUS using the user-defined subroutine UMATHT of Ref. [15]. The FEM mesh consists of 7600 20-noded brick elements (quadratic) and 35,514 nodes. The mesh discretization is summarized in Table 2. The FEM mesh is shown in Fig. 19, which is intended simply to provide a reference solution against which the BEM results can be

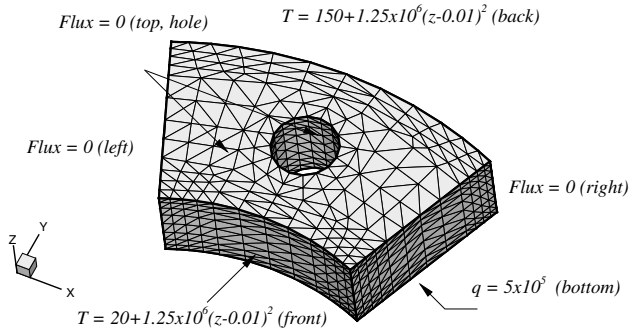

Fig. 18. Thermal boundary conditions and the BEM mesh on the rotor.

Table 2
Mesh discretization by means of BEM and FEM for the rotor problem

Method	Nodes	Elements	Element type
BEM	3492	1584	T6
FEM	35,514	7600	B20

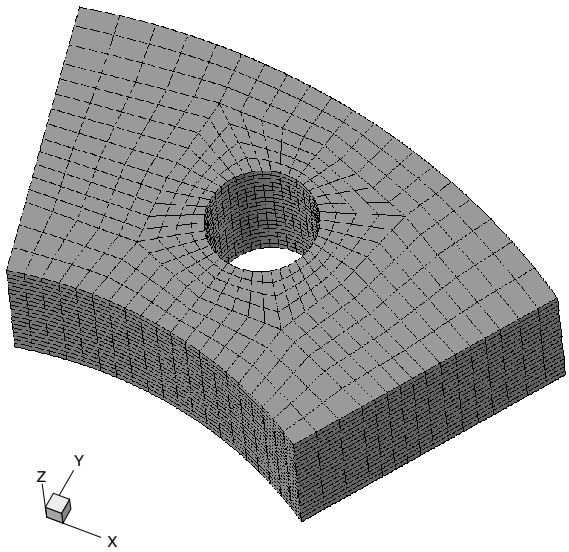

Fig. 19. The FEM mesh with 7600 20-noded brick elements and 35,514 nodes.

compared to. The temperature along the radial direction at the straight edge located at $z = 0.01$ is plotted and compared with the FEM results at different times in Fig. 20. Fig. 21 shows the comparison of the BEM and FEM results for the temperature around the hole at different times. Contour plots of the temperature

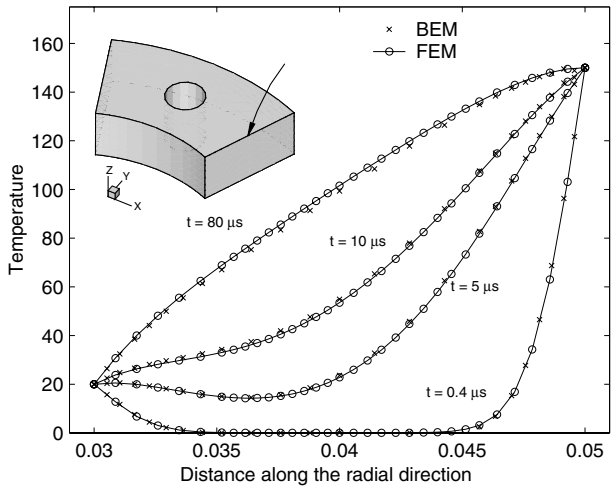

Fig. 20. Temperature distribution along the right top edge (indicated by the arrow).

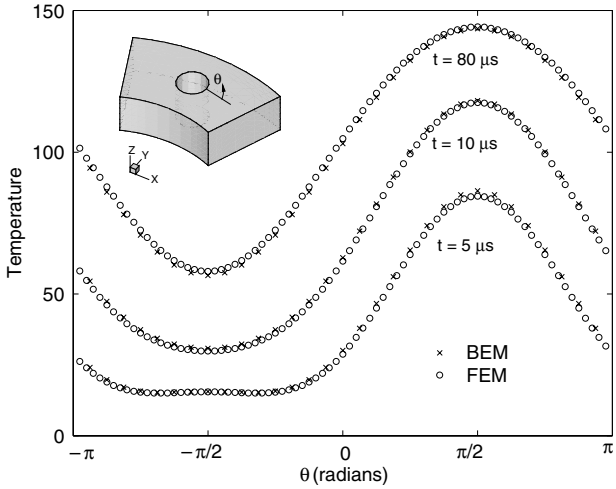

Fig. 21. Temperature distribution along the circular contour around the hole on the top face.

distribution at different time levels are shown in Fig. 22. The radial heat flux at the right interior corner is plotted at various times in Fig. 23. All the results obtained with BEM and the FEM are in good agreement.

7. Conclusions

By means of a simple variable transformation, transient heat conduction problems in functionally graded materials for three different classes of material variation (quadratic, exponential, trigonometric) can be transformed into the homogeneous diffusion problem. Moreover, the material variation can be in one, two or three dimensions. With easy changes in an existing BEM code for homogeneous materials, the FGM

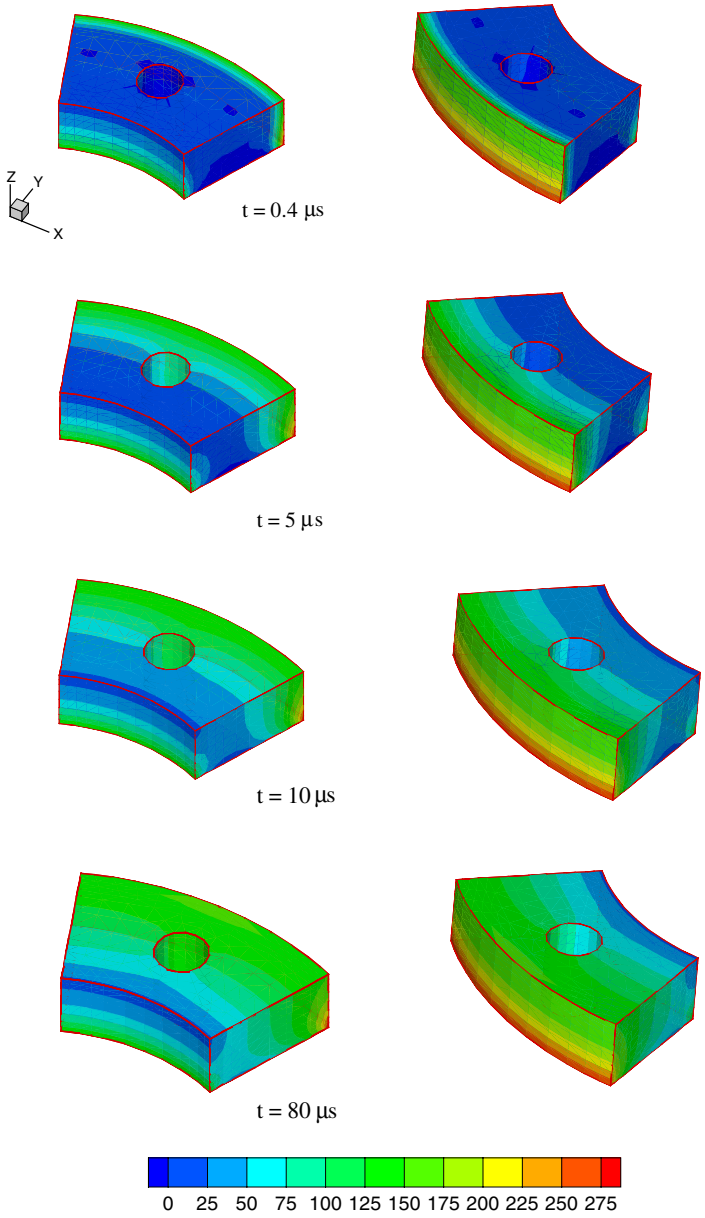

Fig. 22. BEM contour plot of the temperature of the rotor at different time levels.

transient heat conduction problem with constant diffusivity can be solved. A Laplace transform Galerkin BEM formulation has been presented in order to implement the methodology, however, the idea is also applicable to collocation BEM, symmetric Galerkin BEM or meshless BEM. The results of the present BEM numerical simulations show excellent agreement with analytical solutions and FEM simulations. The numerical inversion of the Laplace transform using Stehfest algorithm yield accurate results. Future work involves extension to crack problems.

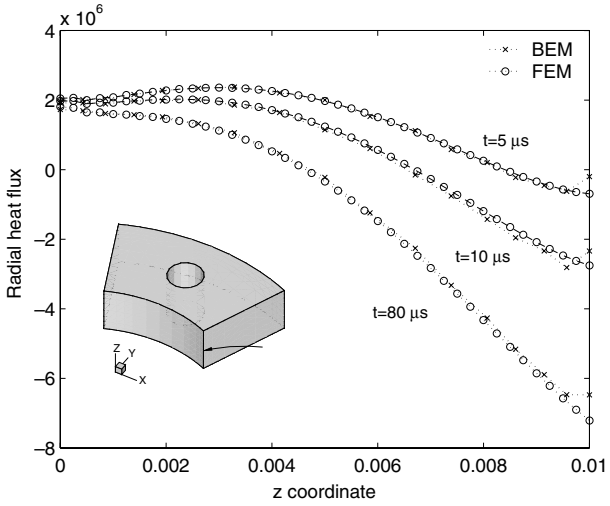

Fig. 23. Radial heat flux along the interior edge (indicated by the arrow).

Acknowledgements

We acknowledge the support from the Computational Science and Engineering (CSE) Program (Prof. Michael Heath, Director) at the University of Illinois at Urbana-Champaign (UIUC) for the CSE Fellowship award to A. Sutradhar. G.H. Paulino acknowledges the support from the National Science Foundation under grant CMS-0115954 (Mechanics and Materials Program).

References

[1] E.M. Carrillo-Heian, R. Douglas Carpenter, G.H. Paulino, J.C. Gibeling, Z.A. Munir, Dense layered $MoSi_2$/SiC functionally graded composites formed by field activated synthesis, J. Am. Ceram. Soc. 84 (2001) 962–968.
[2] Y. Miyamoto, W.A. Kaysser, B.H. Rabin, A. Kawasaki, R.G. Ford, Functionally Graded Materials: Design, Processing and Applications, Kluwer Academic Publishers, Dordrecht, 1999.
[3] S. Suresh, A. Mortensen, Fundamentals of Functionally Graded Materials, The Institute of Materials, IOM Communications Ltd., London, 1998.
[4] G.H. Paulino, Z.H. Jin, R.H. Dodds Jr., Failure of functionally graded materials, in: B. Karihaloo, W.G. Knauss (Eds.), Comprehensive Structural Integrity, vol. 2, Elsevier Science, 2003, pp. 607–644, Chapter 13.
[5] L.C. Wrobel, C.A. Brebbia (Eds.), Boundary Element Methods in Heat Transfer, Computational Mechanics Publication and Elsevier Applied Science, 1992.
[6] A. Sutradhar, G.H. Paulino, L.J. Gray, Transient heat conduction in homogeneous and nonhomogeneous materials by the Laplace transform Galerkin boundary element method, Engrg. Anal. Boundary Elem. 26 (2002) 119–132.
[7] R. Bialecki, G. Kuhn, Boundary element solution of heat conduction problems in multizone bodies of nonlinear materials, Int. J. Numer. Methods Engrg. 36 (1993) 799–809.
[8] E. Divo, A.J. Kassab, Boundary Element Method for Heat Conduction: with Applications in Non-Homogeneous Media, Topics in Engineering Series, vol. 44, WIT Press, Billerica, MA, 2002.
[9] R.P. Shaw, G.D. Manolis, Two dimensional heat conduction in graded materials using conformal mapping, Commun. Numer. Methods Engrg. 19 (2003) 215–221.
[10] M. Tanaka, T. Matsumoto, Y. Suda, A dual reciprocity boundary element method applied to the steady-state heat conduction problem of functionally gradient materials, Electron. J. Boundary Elem. 1 (2002) 128–135.
[11] L.J. Gray, T. Kaplan, J.D. Richardson, G.H. Paulino, Green's functions and boundary integral analysis for exponentially graded materials: heat conduction, ASME J. Appl. Mech. 70 (2003) 543–549.

[12] J. Sladek, V. Sladek, Ch. Zhang, A local BIEM for analysis of transient heat conduction with nonlinear source terms in FGMs, Engrg. Anal. Boundary Elem. 28 (2004) 1–11.
[13] J. Sladek, V. Sladek, Ch. Zhang, Transient heat conduction analysis in functionally graded materials by the meshless local boundary integral equation method, Comput. Mater. Sci. 28 (2003) 494–504.
[14] J. Sladek, V. Sladek, J. Krivacek, Ch. Zhang, Local BIEM for transient heat conduction analysis in 3-D axisymmetric functionally graded solids, Comput. Mech. 32 (2003) 169–176.
[15] A. Sutradhar, G.H. Paulino, A simple boundary element method for potential problems in nonhomogeneous media, Int. J. Numer. Methods Eng., in press.
[16] K.A. Khor, Y.W. Gu, Thermal properties of plasma-sprayed functionally graded thermal barrier coatings, Thin Solid Films 372 (2000) 104–113.
[17] H.S. Carslaw, J.C. Jaeger, Conduction of Heat in Solids, second ed., Clarendon Press, Oxford, 1959, p. 414.
[18] A.H.-D. Cheng, Darcy's flow with variable permeability: a boundary integral solution, Water Resour. Res. 20 (1984) 980–984.
[19] A.H.-D. Cheng, Heterogeneities in flows through porous media by the boundary element method, in: C.A. Brebbia (Ed.), Topics in Boundary Element Research, Applications in Geomechanics, vol. 4, Springer-Verlag, 1987, pp. 129–144, Chapter 6.
[20] R.P. Shaw, Green's functions for heterogeneous media potential problems, Engrg. Anal. Boundary Elem. 13 (1994) 219–221.
[21] R.P. Shaw, G.S. Gipson, Interrelated fundamental solutions for various heterogeneous potential, wave and advective–diffusive problems, Engrg. Anal. Boundary Elem. 16 (1995) 29–34.
[22] K. El Harrouni, D. Quazar, L.C. Wrobel, C.A. Brebbia, Dual reciprocity boundary element method for heterogeneous porous media, in: C.A. Brebbia, M.S. Ingber (Eds.), Boundary Element Technology, VII, Computational Mechanics Publication and Elsevier Applied Science, 1992, pp. 151–159.
[23] K. El Harrouni, D. Quazar, L.C. Wrobel, A.H.-D. Cheng, Global interpolation function based DRBEM applied to Darcy's flow in heterogenous media, Engrg. Anal. Boundary Elem. 16 (1995) 281–285.
[24] B.Q. Li, J.W. Evans, Boundary element solution of heat convection–diffusion problems, J. Comput. Phys. 93 (1991) 255–272.
[25] A. Sutradhar, G.H. Paulino, L.J. Gray, Symmetric Galerkin boundary element method for heat conduction in a functionally graded materials, Int. J. Numer. Methods Engrg., in press.
[26] L.C. Wrobel, C.A. Brebbia, D. Nardini, The dual reciprocity boundary element formulation for transient heat conduction, Finite Elem. Water Resour. VI, Computational Mechanics Publications, Southampton and Springer-Verlag, Berlin, New York, 1986.
[27] Marc S. Ingber, Andrea A. Mammoli, Mary J. Brown, A comparison of domain integral evaluation techniques for boundary element methods, Int. J. Numer. Methods Engrg. 52 (2001) 417–432.
[28] G.H. Paulino, L.J. Gray, Galerkin residuals for error estimation and adaptivity in the symmetric Galerkin boundary integral method, ASCE J. Engrg. Mech. 125 (1999) 575–585.
[29] F. Hartmann, C. Katz, B. Protopsaltis, Boundary elements and symmetry, Ingenieur-Arch. 55 (1985) 440–449.
[30] S.M. Hölzer, The symmetric Galerkin BEM for plane elasticity: scope and applications, in: C. Hirsch (Ed.), Numerical Methods in Engineering '92, Elsevier, 1992.
[31] M. Bonnet, G. Maier, C. Polizzotto, Symmetric Galerkin boundary element method, ASME Appl. Mech. Rev. 51 (1998) 669–704.
[32] L.J. Gray, T. Kaplan, 3D Galerkin integration without Stokes' Theorem, Engrg. Anal. Boundary Elem. 25 (2001) 289–295.
[33] L.J. Gray, J. Glaeser, T. Kaplan, Direct evaluation of hypersingular Galerkin surface integrals, SIAM J. Sci. Comput. 25 (2004) 1534–1556.
[34] H. Stehfest, Algorithm 368: numerical inversion of Laplace transform, Commun. Assoc. Comput. Mach. 13 (1970) 19–47.
[35] H. Stehfest, Remarks on algorithm 368: numerical inversion of Laplace transform, Commun. Assoc. Comput. Mach. 13 (1970) 624.
[36] R.S. Nordlund, A.J. Kassab, Non-Fourier heat conduction: a boundary element solution of the hyperbolic heat conduction equation, in: C.A. Brebbia, S. Kim, T. Osswald, H. Power (Eds.), BEM17: Proceedings of the 17th International Conference on Boundary Elements, Computational Mechanics Publications, 1995, pp. 279–286.
[37] G.J. Moridis, D.L. Reddell, The Laplace transform boundary element (LTBE) method for the solution of diffusion-type equations, in: C.A. Brebbia, G.S. Gipson (Eds.), BEM XIII, Computational Mechanics Publications, 1991, pp. 83–97.
[38] S.P. Zhu, P. Satravaha, X. Lu, Solving the linear diffusion equations with the dual reciprocity methods in Laplace space, Engrg. Anal. Boundary Elem. 9 (1994) 39–46.
[39] ABAQUS Version 6.2. Hibbitt, Karlsson and Sorensen, Inc. Pawtucket, RI, USA, 2002.
[40] M.H. Santare, J. Lambros, Use of graded finite elements to model the behavior of nonhomogeneous materials, ASME J. Appl. Mech. 67 (2000) 819–822.
[41] J.-H. Kim, G.H. Paulino, Isoparametric graded finite elements for nonhomogeneous isotropic and orthotropic materials, ASME J. Appl. Mech. 69 (2002) 502–514.
[42] M.C. Walters, G.H. Paulino, R.H. Dodds Jr., Stress intensity factors for surface cracks in functionally graded materials under mode I thermomechanical loading, Int. J. Solids Struct. 41 (2004) 1081–1118.